



# Non-Quasi-Static modeling and methodology in fully depleted SOI MOSFET for L-UTSOI model<sup>☆</sup>

S. Martinie<sup>a,\*</sup>, O. Rozeau<sup>a</sup>, HyoEun Park<sup>b</sup>, Sungjoon Park<sup>b</sup>, P. Scheer<sup>c</sup>, S. El Ghouli<sup>c</sup>, A. Juge<sup>c</sup>, H. Lee<sup>b</sup>, T. Poiroux<sup>a</sup>

<sup>a</sup> Univ. Grenoble Alpes, CEA, LETI, F-38000 Grenoble, France

<sup>b</sup> Samsung, South Korea

<sup>c</sup> STMicroelectronics Crolles, France

## ARTICLE INFO

### Keywords:

NQS  
L-UTSOI  
Compact model  
SPICE  
FDSOI

## ABSTRACT

With the maturity of CMOS technologies and their use for various digital, analog and RF applications, some additional effects must be modeled or enhanced to improve the accuracy of SPICE models. Non-Quasi-Static (NQS) effect is one of them; this paper proposes here to present a pragmatic NQS approach adapted to L-UTSOI model and compared to TCAD simulation, segmented model and experimental data.

## 1. Introduction

The Fully-Depleted Silicon On Insulator (FDSOI) technologies are deployed for a wide range of Radio Frequency (RF) applications at high frequency operation. Usually, the surface potential based compact models of MOSFET (implemented in SPICE) are built within the Quasi-Static (QS) approximation, which means that continuity equation has no temporal dependence and consequently carriers are not dynamically affected along the channel. This paper describes the recent improvements of L-UTSOI standard model by the adaptation of the Non-Quasi-Static Relaxation Time Approximation (NQS-RTA) model from literature [1–3] to enhance it. This new feature has been validated and confronted to the TCAD simulation, segmented model methodology (which is the usual SPICE technique to include very accurately NQS effect) and silicon experimental data.

The paper is organized as follows. In Section 2, we focus on the review of different techniques, which are the main motivation of the choice of NQS-RTA approach. In Section 3, we present the new physical insights included in L-UTSOI model version relative to NQS effect. Finally, Section 4, NQS-RTA solution is formally illustrated, discussed and compared with TCAD, segmented case and experimental datas.

## 2. NQS SPICE modeling: between complexity and efficiency

Under a high-frequency operation, the charge modulation in MOSFET may no longer follow the signal instantaneously, leading to a

so-called Non-Quasi-Static (NQS) effect. It has been largely explored in literature for SPICE, analytical or small-signal modeling where different models or methodologies have been proposed [1–9].

From a SPICE model usage point of view, the most accurate solution is to break down the MOSFET in  $N$  equal channel segments using an appropriate methodology for parameter setting and physical effects activation [7,8]. Independently of the runtime that is, strictly speaking, dependent of the number of transistors (i.e. segments) solved in SPICE netlist, the main limitation of the segmented model is the parameter extraction adapted to all physical phenomena (such as SCE, DIBL, GIDL, saturation velocity ...) that cannot be topologically segmented (such as low field mobility). For example, constant part of source or drain resistance is externally set (RSW1 parameter in L-UTSOI [10] is replaced by external resistance at source and drain of equivalent circuit), but the corresponding voltage dependencies are more difficult to handle (RSGO parameter in L-UTSOI [10]).

Another method is the spline collocation-based approach [4,5] where the 1D current continuity equation is solved. In practice, the user chooses the number of channel partitions that defines the number of collocation points. The channel charge density is then approximated by a cubic spline through these collocation points. Each collocation point (up to 9 in PSP model through SWNQS parameter [5]) corresponds to an additional RC branch where an equivalent number of internal nodes (in addition to modeling equation) is necessary to achieve a good accuracy with respect to the segmented model. Even if the

<sup>☆</sup> The review of this paper was arranged by Francisco Gamiz.

\* Corresponding author.

E-mail address: [sebastien.martinie@cea.fr](mailto:sebastien.martinie@cea.fr) (S. Martinie).

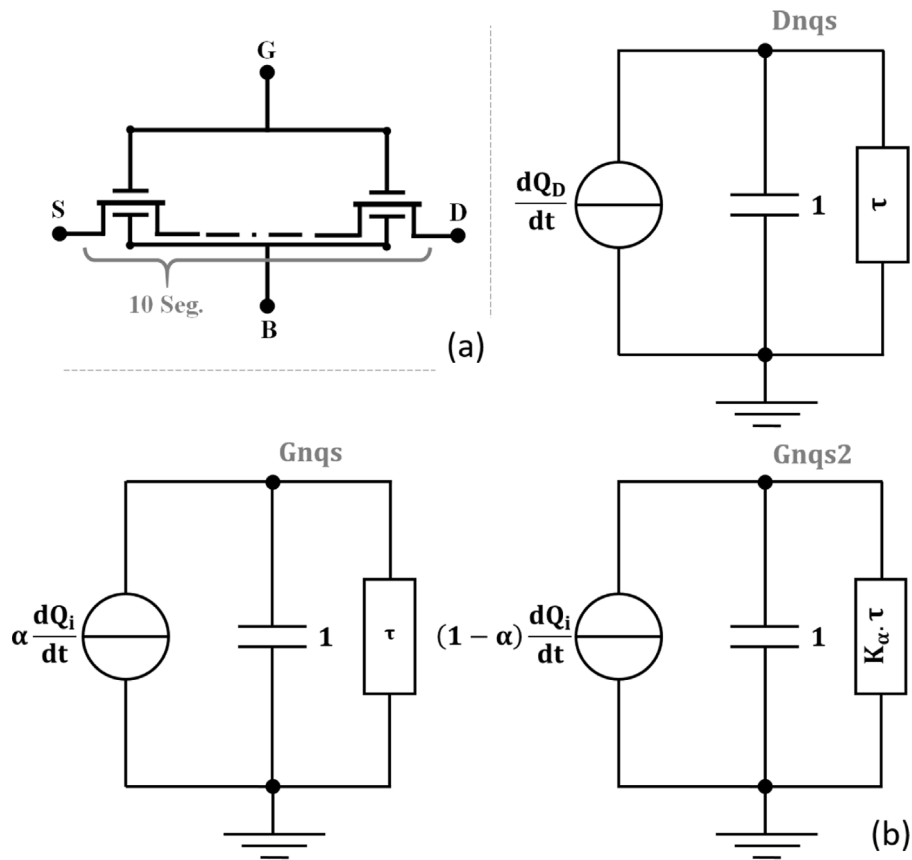


Fig. 1. (a) segmented topology and (b) equivalent circuit used to emulate NQS-RTA model and superimposed to the MOSFET.

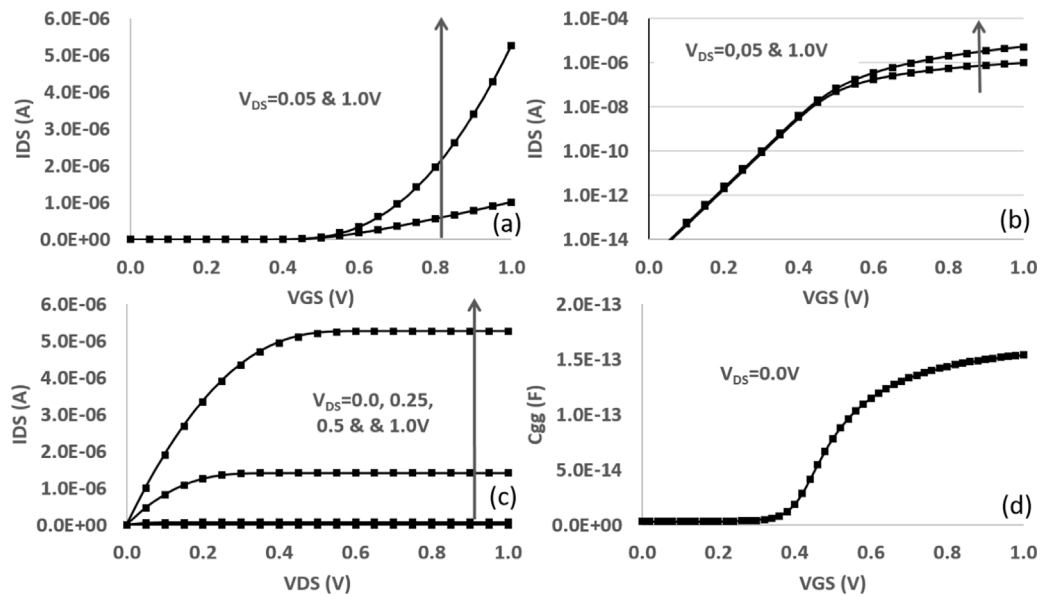


Fig. 2. Validation of segmented model (line) with TCAD (symbol) for long and wide device ( $W = L = 1 \mu m$ ,  $T_{ox} = 2 \text{ nm}$ ,  $T_{si} = 10 \text{ n}$  and  $T_{box} = 25 \text{ n}$ ). linear and saturate  $I_{DS}$  vs  $V_{GS}$  in lin. (a) and log. (b) scale, (c)  $I_{DS}$  vs  $V_{DS}$  for different  $V_{GS}$  and (d)  $C_{gg}$  vs  $V_{GS}$  at 10 kHz.

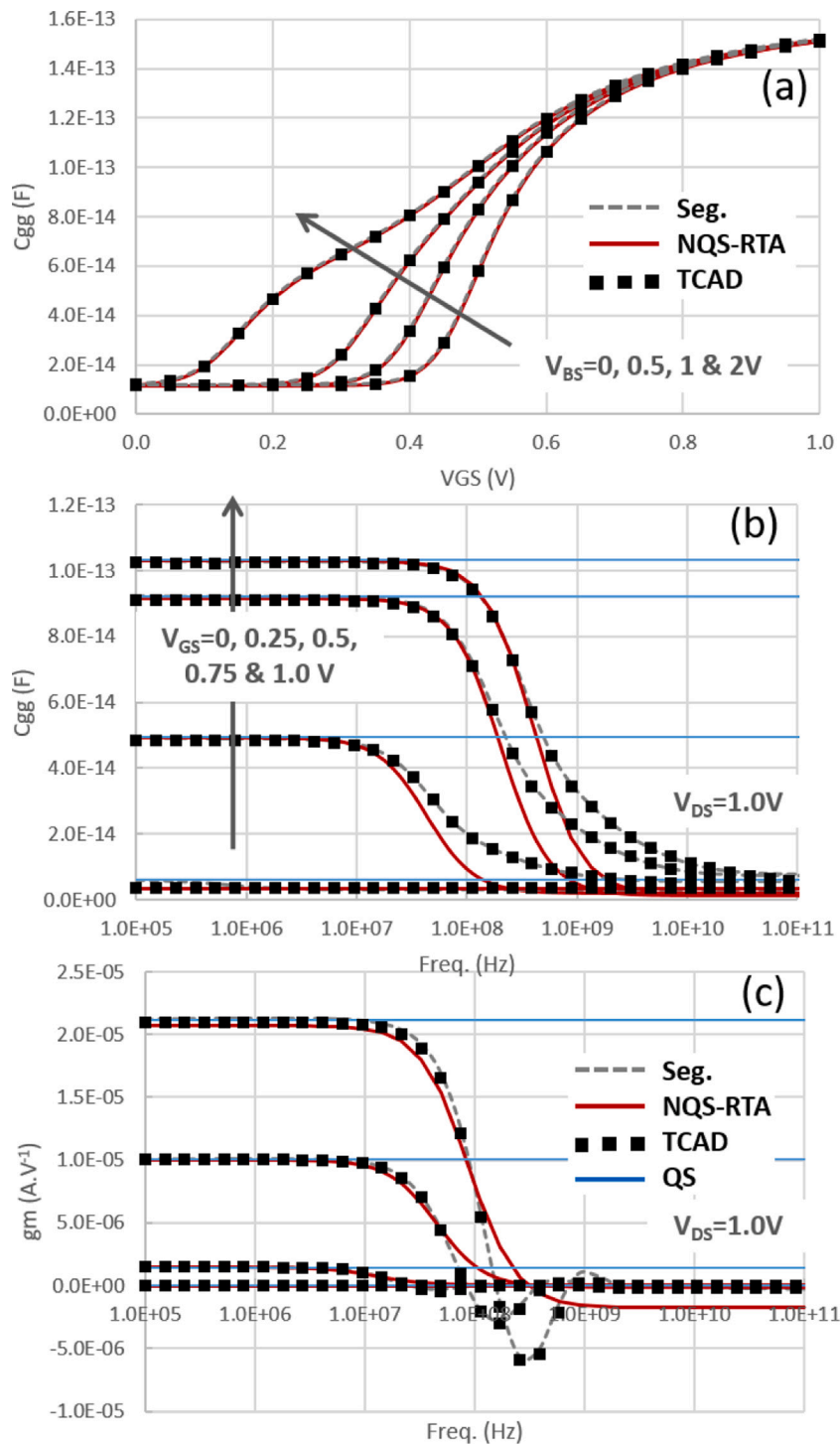


Fig. 3. Comparison between TCAD (symbol), segmented (dashed line) and NQS-RTA model (line) for long and wide device ( $W = L = 1 \mu m$ ,  $T_{ox} = 2 nm$ ,  $T_{si} = 10n$  and  $T_{box} = 25n$ ). (a) TCAD, seg. and NQS-RTA  $C_{gg}$  vs  $V_{GS}$  and  $V_{BS}$  (Freq. = 10 kHz), 2 port S-parameter TCAD, Quasi-Static (QS), seg. and NQS-RTA (b)  $C_{gg} = \text{imag}(Y_{11})/2.\pi.f$  and (c)  $g_m = \text{real}(Y_{21}-Y_{12})$ .

parameter extraction is not affected (only extra mobility parameter MUNQS is used for the transition frequency modulation), the spline collocation-based approach is difficult to apply to models such as L-UTSOI without compromising the runtime efficiency and the robustness of the simulations.

Finally, the most popular simplified approach is the use of Relaxation Time Approximation (RTA), which reduces the extra runtime and improves convergence, but with lower accuracy [1–3]. The principle is

to use an extra subcircuit to have direct translation of RTA equation into basic circuit element (parallel RC network) where the node gives the value of the time dependent charge (modulate by the time constant or relaxation time  $\tau$ ). With this approach, only one additional node is required and the topology of transistor and QS calculation is preserved at low frequency. Initial implementation [1,2] used a QS calculation of the partition from the inversion charge to drain charge, but as explained in [3], it is more efficient to apply the RTA to both the inversion and

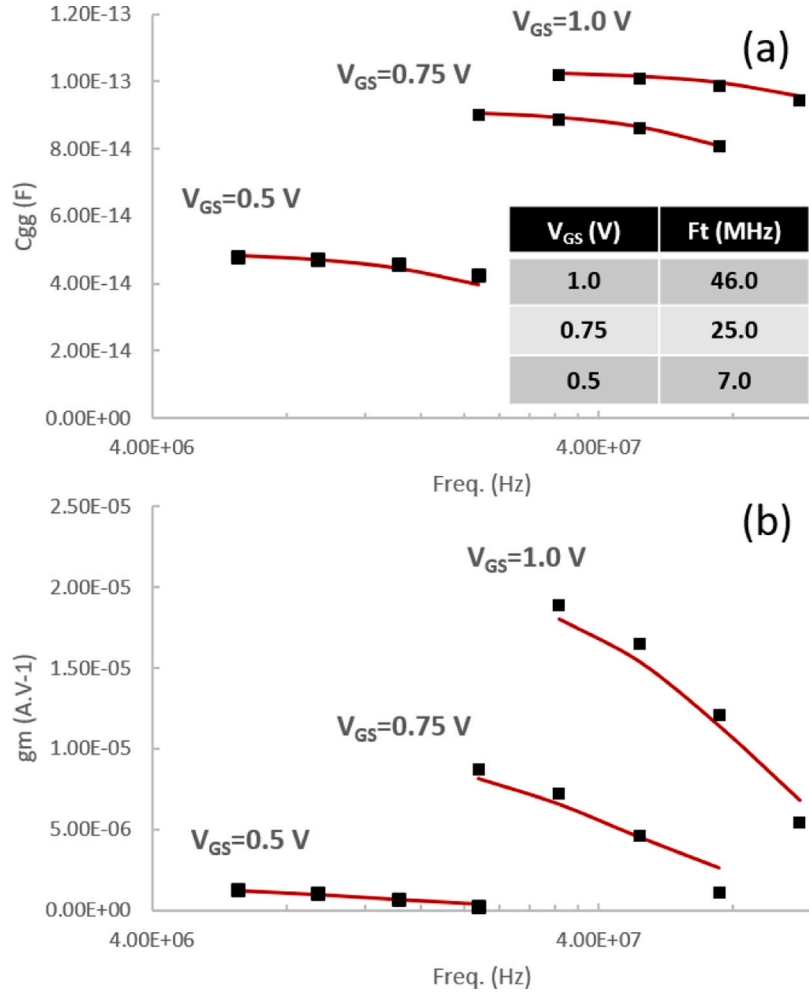


Fig. 4. Comparison between TCAD (symbol) and NQS-RTA model (line) around the transition frequency ( $F_t$ ) for long and wide device ( $W = L = 1 \mu\text{m}$ ,  $T_{ox} = 2 \text{ nm}$ ,  $T_{si} = 10 \text{ nm}$  and  $T_{box} = 25 \text{ nm}$ ). 2 port S-parameter TCAD and NQS-RTA (b)  $C_{gg} = \text{imag}(Y_{11})/2\pi.f$  and (c)  $g_m = \text{real}(Y_{21}-Y_{12})$ .

drain charges. This is to avoid any trouble by introducing intermediate extra calculation of QS partition of the total inversion charge on drain charge.

The limitation of this approach is his own empirical view of NQS effect through one RC network. Physically NQS effect should not only model through unique relaxation time over the whole frequency range operation as explained in [1–3]. Even if corresponding relaxation model include drift and diffusion part to capture polarization dependence; this is not sufficient for whole frequency variation.

### 3. Segmented and RTA model in L-UTSOI

L-UTSOI is the first available standard compact model able to describe the behavior of an ultra-thin body and BOX FDSOI transistor including strongly inverted back interface [10,11]. Regarding NQS modeling, we firstly illustrate the segmented model case with ten segments (cf. fig 1.a) by using similar methodology as [7]. In practice for L-UTSOI, several parameters of each device's segment are similar as initial model or simply scaled with respect to the number of segments  $N$  (i.e.  $L_{seg} = L/N$ ). The most critical point is the adaptation to other non-segmentable feature as mentioned earlier (velocity saturation or channel length modulation). This means that the value of each parameter extracted on initial device vs segmented device is not the same or/and there are no segmentation rule.

As depicted in Fig. 2, we reproduce exactly the TCAD [12] simulation results on the DC and CV. Likewise as illustrated on Fig. 3, we reproduce also accurately the frequency dependent figures of merit for large frequency.

However, as explained in the previous part, this approach has some limitations (runtime due to multiplication of model instances, complexity in parameters extraction strategy ...). Thus, we propose to use the NQS-RTA in L-UTSOI. The global topology is illustrated in Fig. 1.b where the corresponding RTA equations is solved for  $Q_i$  and  $Q_D$  by the circuit simulator thanks to the use of internal nodes:

$$\frac{\partial Q_x}{\partial t} = -\frac{Q_x - Q_x^{QS}}{\tau} \quad (1)$$

where  $Q_x$  is charge at node  $x$ , QS index is for Quasi-Static and  $\tau$  is the relaxation time. The relaxation time is given by Eq. (2) similar to [2-3]:

$$\frac{1}{\tau} = \frac{\mu_{eff}}{L} \left( K_{DRIFT} \cdot \frac{Q_i}{C_{ox}} + K_{DIFF} \cdot u_t \right) \quad (2)$$

where  $\mu_{eff}$  is the low field mobility,  $L$  is the channel length,  $C_{ox}$  is the oxide capacitance,  $Q_i$  is the inversion charge,  $u_t$  is the thermal voltage and  $K_{DRIFT}$  &  $K_{DIFF}$  are model parameters corresponding to the drift and diffusion current components.

An empirical pole is added to improve a little bit the accuracy through the partition parameter  $\alpha \in [0,1]$  with an associated relaxation

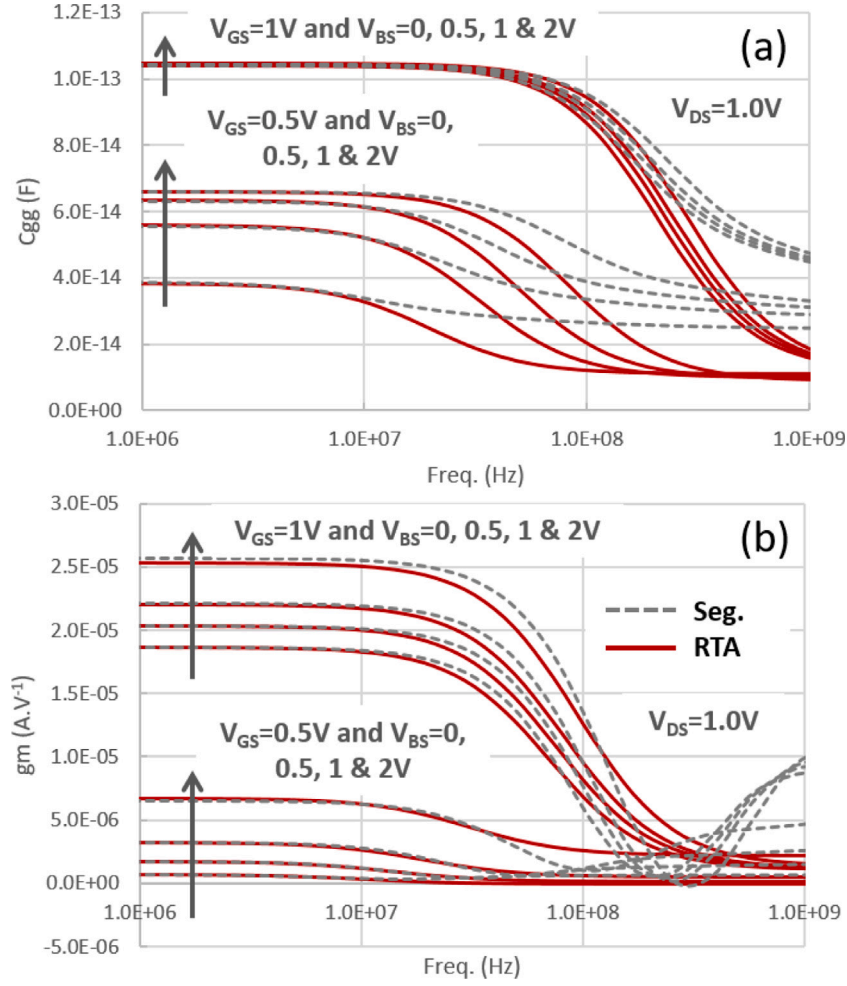


Fig. 5. Comparison between segmented (dashed line) and NQS-RTA model (line) for long and wide device ( $W = L = 1 \mu\text{m}$ ,  $T_{\text{ox}} = 2 \text{ nm}$ ,  $T_{\text{si}} = 10 \text{ nm}$  and  $T_{\text{box}} = 25 \text{ nm}$ ). (a)  $C_{\text{gg}} = \text{imag}(Y_{11})/2\pi \cdot f$  and (b)  $g_m = \text{real}(Y_{21}-Y_{12})$ .

time  $K_{\alpha}$ . Thus, Eqs. (3) and (4) represent the final temporal part of the terminal currents:

$$I_{DS} \propto -\frac{1}{\tau} \cdot V(D_{nqs}) \quad (3)$$

$$I_{GS} \propto -\frac{1}{\tau} \cdot \left( V(G_{nqs}) + \frac{V(G_{nqs2})}{K_{\alpha}} \right) \quad (4)$$

where  $D_{nqs}$ ,  $G_{nqs}$  and  $G_{nqs2}$  represent nodes of equivalent circuit in Fig. 1.b.

#### 4. Simulation results and discussion

Following the equivalent circuit, the global implementation of the model is reachable and one has only to care about the collapse of the internal node when NQS is deactivated to avoid any extra runtime. Fig. 3.b and 3.c illustrate clearly the good accuracy of NQS-RTA model up to twice the transition frequency. Specifically Fig. 4 illustrates the comparison between TCAD and NQS-RTA model around transition frequency to highlight the compromise of such solution. Interestingly on Fig. 5.a and 5.b, the model is also able to capture the back bias dependence, including the back channel inversion charge since the inversion charge ( $Q_i$ ) naturally includes this effect as well as the low field mobility ( $\mu_{eff}$ ). Note that global extraction strategy is: firstly extract QS current and charge ( $T_{\text{OX}}$ ,  $T_{\text{BOX}}$ , fringing capacitance ... on CV and mobility, SCE, DIBL ... on current) and secondly using KDRIFT, KDIFF parameter to extract frequency dependence.

Fig. 6 is a comparison on long and wide experimental device on 28 nm FDSOI. We show here for a full range of  $V_{DS}$  and  $V_{GS}$ , the capability of the NQS-RTA model to reproduce measurements. Note that QS extraction (low frequency) is not illustrated here through IV and CV, but follows the usual extraction flow, only KDRIFT and KDIFF are extracted on the frequency dependence figure of merits. Note that in practice these 2 NQS related parameters have geometrical dependence to ensure a good model scalability.

Fig. 7 shows the simulation of “killer” NOR gate circuit which is a good benchmark of interest for NQS effect [4] and to illustrate the effect of such model on transients. The large peak, observed in QS condition due to a non physical current from the top transistor, is strongly reduced when we use the NQS model. As expected, this peak modulation is directly dependent on the model’s parameters setting (KDRIFT and KDIFF).

Even if only longer channel are illustrated in present paper, this comparison is done to have a clear view of NQS-RTA model’s limitations against TCAD. As expected for shorter channels, transition frequency increases and comparison is more favorable.

#### 5. Conclusion

In this paper, we have presented the recent enhancements brought to L-UTSOI model to enlarge his capability for RF applications. Starting



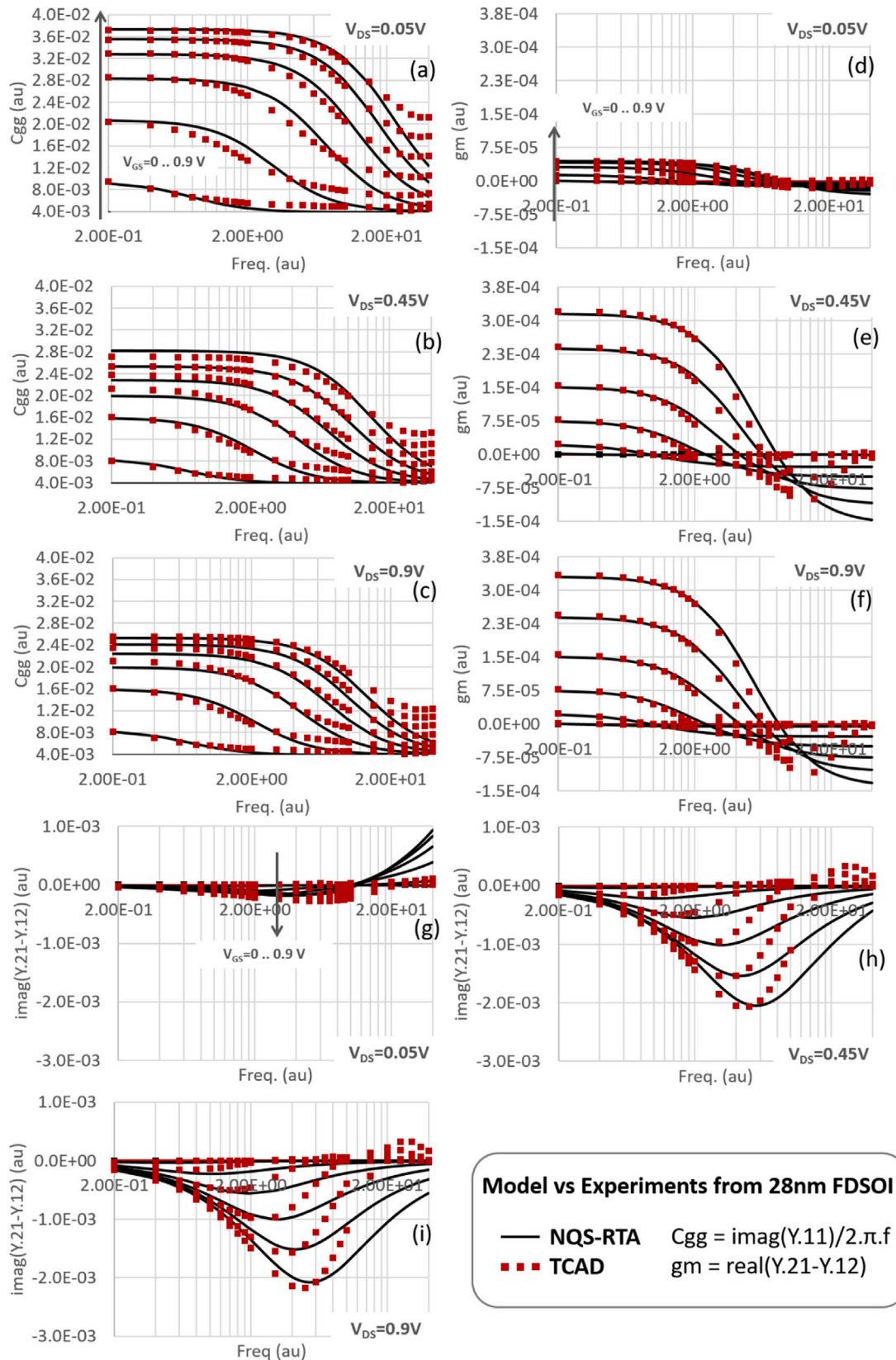


Fig. 6. Normalized experiments from 28 nm technology (symbol) vs NQS-RTA model (line) for long and wide device on 2 port S-parameter measurement and simulation: Gm =  $\text{real}(Y_{21}-Y_{12})$ , Cgg =  $\text{imag}(Y_{11})/2\pi.f$  and  $\text{imag}(Y_{21}-Y_{12})$  vs Frequency for VGS = 0.0 .. 0.9 V at VDS = 0.05 V (a, d and g), VDS = 0.45 V (b, e and h) and VDS = 0.9 V (c, f and i).

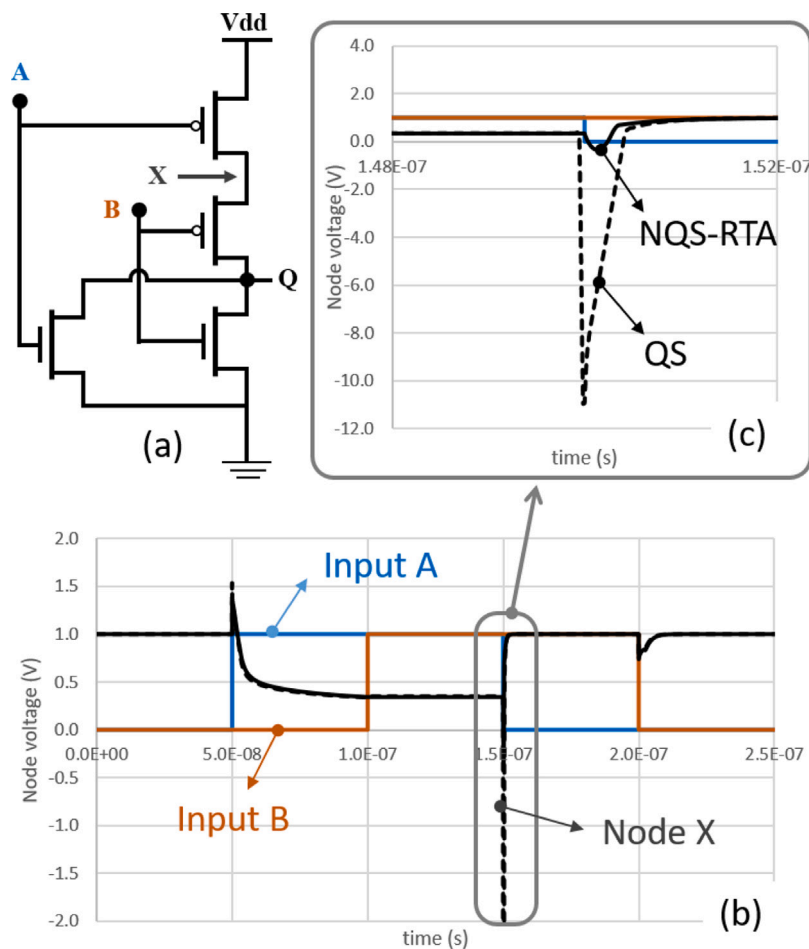


Fig. 7. Practical illustration of NQS-RTA model on circuit simulation. (a) “Killer” NOR Gate circuit used to illustrate the interest of NQS-RTA model, (b) comparison of the simulated voltage at node X of the killer NOR gate using the Quasi-Static (QS without any frequency dependence) and the NQS-RTA models and (c) zoom on the glitch itself.

from presentation of different technique to mimic NQS effect in SPICE modeling, we chose to adapt the well-known NQS-RTA approach.

By comparison with segmented model and experimental data, we have illustrated the frequency dependence limitation and accuracy of such model. As mentioned in previous paper this approach is a first order solution [1–3], the successful adaptation of NQS-RTA model in L-UTSOI is the right compromise between runtime, accuracy and simplicity in comparison to the segmented model, while preserving the description of back interface inversion. Note that NQS-RTA implementation is an “end of code” modification which is relatively “light” in term of implementation. Simulations of 11 stages Ring Oscillator Fan-Out 4 on different SPICE simulators with same library given same frequency shows an average runtime increase around 20%.

#### Declaration of competing interest

The authors declare the following financial interests/personal relationships which may be considered as potential competing interests: Sébastien Martinie.

#### Data availability

The authors are unable or have chosen not to specify which data has been used.

#### References

- [1] Chan M, Hui KY, Hu C, Ko PK. A robust and physical BSIM3 non-quasi-static transient and AC small-signal model for circuit simulation. *Trans Electron Dev* 2006;45(4).
- [2] Navarro D, Takeda Y, Miyake M, Nakayama N, Machida K, Ezaki T, et al. A carrier-transit-delay-based nonquasi-static MOSFET model for circuit simulation and its application to harmonic distortion analysis. *Trans Electron Dev* 2006;53(9).
- [3] Zhu Z, Gildenblat G, McAndrew Colin C, Lim Ik-Sung. Accurate RTA-based nonquasi-static MOSFET model for RF and mixed-signal simulations. *Trans Electron Dev* 2012;59(5).
- [4] Wang H, Li Xin, Wu W, Gildenblat G, van Langevelde R, Smit GDJ, et al. A unified nonquasi-static MOSFET model for large-signal and small-signal simulations. *Trans Electron Dev* 2006;53(9).
- [5] PSP 103.7 Verilog-A and documentation. <http://www.cea.fr/cea-tech/leti/pspsupport>.
- [6] Porret A-S, Sallèse J-M, Enz CC. A compact non-quasi-static extension of a charged-based MOS model. *Trans Electron Dev* 2001;48(8).
- [7] Scholten AJ, Tiemeijer LF, De Vreede PWH, Klaassen DBM. A large signal non-quasi-static MOS model for RF circuit simulation. In: *International electron devices meeting*. 1999.
- [8] Bucher M, Bazigos A. An efficient channel segmentation approach for a large-signal NQS MOSFET model. *Solid-State Electron* 2008;52:275–81.
- [9] Bagheri M, Tsvividis Y. A small signal DC-to-high-frequency nonquasi-static model for the four-terminal MOSFET valid in all regions of operation. *Trans Electron Dev* 1985;ED-32(11).
- [10] Poiroux T, Rozeau O, Scheer P, Martinie S, Jaud M-A, Minondo M, et al. Leti-UTSOI2.1: A compact model for UTBB-FDSOI technologies—Part II: DC and AC model description. *Trans Electron Dev* 2015;62(9).
- [11] L-UTSOI 103.5 Verilog-A and documentation <https://www.cea.fr/cea-tech/leti/1-utsoisupport>.
- [12] TCAD Sentaurus Device Manual, Synopsys, Inc.: Q-2019.12.